Наведено результати експериментальних досліджень розподілу температури на поверхні металевого гофрованого листа.

Запропоновано математичні моделі для розрахунку теплопровідності та термонапруженого стану фрагмента металевої гофрованої оболонки транспортної споруди, бокові поверхні якої нагріті до різних температур. Приймається, що температура залежить від двох просторових змінних. В якості можливого критерію для вибору потрібної функції розподілу температури спорудою прийнято мінімізацію функціоналу, визначеного на множині допустимих функцій, у вигляді інтегралу по області тіла від виразу, що задає виробництво ентропії.

При дослідженні температурного поля використовується диференціальне рівняння теплопровідності, а напружено-деформованого стану – рівняння теорії термопружності. Для розв'язування диференціального рівняння теплопровідності використано метод скінченних різниць, а для розв'язку рівнянь теорії термопружності – метод скінченних елементів.

Встановлено, що температура розподіляється нерівномірно металевим гофрованим листом. Існує температурний перепад між нижньою та верхньою поверхнями гофрованого металевого листа. Різниця температур між нижньою та верхньою поверхнями листа становить +7,1 °С при максимальних додатних температурах навколишнього середовища та –5,5 °С при мінімальних від'ємних температурах навколишнього середовища.

Встановлено, що величина напружень, яка виникає в металевих гофрованих листах від температурних перепадів навколишнього середовища, становить до 25 % від допустимих напружень. Тому при проектуванні металевих гофрованих конструкцій необхідно проводити розрахунок на дію температурних кліматичних впливів.

Отримані дані термонапруженого стану металевих гофрованих конструкцій є важливими для проектних організацій. Оскільки із врахуванням дії температурного поля на напружений стан конструкції в цілому на стадії проектування можна підібрати матеріали з метою зменшення температурних напружень, які мають прямий вплив на розвиток корозійного пошкодження металу труби

Ключові слова: металева гофрована оболонка, розподіл температури, температурне поле, термонапружений стан оболонки

UDC 625.151.2.001.4, 531.01
DOI: 10.15587/1729-4061.2019.168260

A STUDY OF THE EFFECTS OF CLIMATIC TEMPERATURE CHANGES ON THE CORRUGATED STRUCTURE OF A CULVERT OF A TRANSPORTATION FACILITY

B. Gera
Doctor of Technical Sciences, Professor
Department of Transport Technologies*
E-mail: gera-zen@ukr.net
V. Kovalchuk
PhD
Department of Rolling Stock and Track*
E-mail: kovalchuk.diit@gmail.com
*Lviv branch of Dnipropetrovsk National University of Railway Transport named after Academician V. Lazaryan
Dnipro National University of Railway Transport named after Academician V. Lazaryan
Lazariana str., 2, Dnipro, Ukraine, 49010

1. Introduction

Transportation facilities that are made of corrugated metal structures (CMSs) undergo a complex of climatic effects [1, 2] in the process of using them. Research on heat exchange components is an integral part of data development for calculating temperature stresses and deformations.

In winter, the ground is frozen and cooled to significantly low temperatures. As a result of contact with the metal culvert, cracks may occur in the soil, which adversely affects the technical condition of the construction [3, 4]. The formation of cracks in the soil negatively affects the interaction of the pipe with the ground filling, reducing its bearing capacity. If an estimate confirms the possibility of temperature-based cracking of the soil of the embankment above the upper part of the culvert, a heat-insulating layer should be used, the thickness of which should be selected by mathematical modelling in such a way as to reduce the level of temperature stresses.

In addition, during the functioning of corrugated metal structures, cracking of the zinc coating may be observed. One of the reasons for this defect is the level of temperature stresses on the boundaries of «metal – zinc» or «metal – zinc – soil». This is due to the temperature difference between the external heated metal surface of the corrugated sheet construction and the inner part of the structure that interacts with the ground filling and has a lower temperature value. The basis of such a calculation is the prediction of the temperature field and the field of temperature stresses with the help of mathematical modelling.

In this connection, the problem of studying the temperature field and the thermal stress state of corrugated metal pipes that are exposed to changing climatic influences of the envi-

© B. Gera, V. Kovalchuk, 2019

Received date: 22.04.2019 Accepted date: 14.05.2019 Published date: 26.06.2019

ronment is relevant. Such studies, along with researching the impact of static and variable transport loads, are the basis for assessing the strength and reliability of transportation facilities that are made of the CMS when interacting with the ground.

2. Literature review and problem statement

In most cases, it is difficult to determine temperature fields and stresses, and the exact solution of the problem is hard to find. Therefore, an engineer has to simplify the actual design in the calculations and take into account the involved physical factors of the error thus made or use approximate methods of research [5]. It is necessary to take into account the multi-axial stressed state in order to obtain complete data on the tense state of transportation facilities due to climatic temperature effects [6], and it is not enough to solve a one-dimensional problem [7].

In [8–10], it was concluded that fluctuations in the atmospheric temperature cause permanent extensions and shrinkages of beams in long-span bridges, and the temperature difference leads to the appearance of bending moments.

According to the requirements of DBN B.2.3-14 [11], the normative climatic temperature effects must be taken into account when calculating the second-group boundary condition for bridges of all systems. Determination of the design temperatures is based on the normative atmospheric temperature (air temperature in warm and cold periods of the year). It is recommended to determine the temperature of elements with complex cross-section by taking into account the value of the average weighted temperature of individual elements (walls, shelves, etc.).

The average normative temperature in the section of the elements or their parts is recommended to be assumed as equal to:

– the normative atmospheric temperatures for concrete and reinforced concrete elements in the cold period of the year, and for metal constructions – at any time of year;

– the normative atmospheric temperature, except for a value equal to $0.2a$, but not more than 10 °C for concrete and reinforced concrete elements during the warm period of the year. Here, the parameter a is the thickness of an element or part thereof in centimetres, including the road wear of the travel section of road bridges.

The normative document AASHTO [12] lists the limits on the highest and lowest design temperatures for different types of bridges given. These temperature values must be taken into account when designing bridge structures.

When calculating long-span steel reinforced concrete bridges, taking into account uneven heating by the sun and the norms [13], it is necessary to take into consideration nine calculated cases of temperature effects on bridge constructions.

In the normative document EN-1991-1-5-2009 [14], it is recommended to take into account temperature variations in the design of transportation facilities. In this case, it is necessary to check the influence of the highest and lowest temperatures on the thermal stress state of bridge structures.

In [15], it was experimentally established that a seasonal change in the atmospheric temperature influences the occurrence of deformations in the design of the embankment with tunnel treatment. The deformation value differs depending on the heat transfer conditions along the boundaries of the calculated area «soil-tunnel». Under multivariate modelling of the thermal stress state, it is established that with the help of special means that change the conditions of heat exchange on the outer and inner surfaces of the tunnel, it is possible to achieve practical stabilization of the deformed state of the embankment design and thereby improve its performance. It is also noted that the methods of calculating the thermal stress state in the area of culverts are not sufficiently developed. Such processes can be estimated reliably only experimentally.

In [16], it is noted that in order to determine the thermal stress state of a reinforced concrete structure of bridges, it is necessary to know the temperature distribution in the body of the structure. However, the author considers the distribution of the thermal stress state only in the reinforced long-span concrete structures of the bridges.

The authors of [17] found that one of the main reasons for the malfunction of asphalt concrete coatings and slabs of the roadway on road bridges is the influence of temperature, and in [18], it was proved that temperature leads to the asphalt subsidence.

Several specific examples are given for implementing the method for studying the temperature fields [19] and the mechanical stresses [20] arising in the layers of the road surface. However, these studies do not consider issues related to researching temperature distribution with uneven heating of the layers of road coating and their impact on bridge structures.

In [21], when designing transportation facilities, it is also taken into account that there is a temperature distribution in the section of the elements of long-span structures. In this case, the values of both positive and negative gradients are used. For example, when designing the famous San Francisco-Oakland Bay Bridge [21], the following temperature effects were taken: 27 °C as the average temperature; 17 °C as the increase or decrease of temperature for concrete; 22 °C as the increase or decrease of temperature for steel; the temperature gradients for concrete were of two types: positive $T_1=30$ °C and $T_2=7.8$ °C as well as negative $T_1=-15$ °C and $T_2=-3.9$ °C according to the graphs of the AASHTO standards; the temperature difference between the upper and lower surfaces of steel beams was 11 °C.

According to the temperature measurements for a Canadian steel bridge and the subsequent calculations of the thermal stresses [22], it was concluded that the distribution of temperatures in the designs of such bridges should be taken into account when designing the constructions. It is especially important to take into consideration spring temperatures, since the walls of the beams that are facing the sun during this period are heated very quickly while the temperature of the concrete pavement, at the same time, changes slightly.

The results of the temperature distribution on the surfaces of the metal box-beam have shown that the temperature between the upper and lower parts of the box beams is distributed unevenly. The temperature difference reaches a value greater than 24 °C [23].

In [24], the influence of temperatures on the dynamic behaviour of bridges is analysed, and a model for determining the degree of damage to box-type bridge structures with temperature influences is developed.

The results of experimental measurements of temperature distribution on the surfaces of bridge structures are presented for 4 years in [25]. After performing the measurements, a conclusion was made that the thermal gradients that occur on the bridges are inevitable in the process of monitoring the stress-strain state of the bridge structures. The temperature measurement should always be carried out simultaneously with the measurement of deflections. Moreover, attention should be paid to the atmospheric temperature and weather conditions.

In Germany, when evaluating thermal effects on long-span metal structures of box bridges, due to the effect of atmospheric temperature, a computer model was developed. It was based on taking into account all external climatic influences and material parameters for heat transfer, which influence the temperature distribution throughout the beams.

The results of calculating temperature gradients given in [26] show that the section direction in the vertical direction of the beam is distributed unevenly. Between the bottom and the upper edge of the beam, there is a temperature difference ΔT. In this case, the horizontal or equivalent temperature differences between the lateral edges of the beam can be obtained from each temperature distribution, taking into account concrete cross-sectional shapes.

From the analysis made, it can be noted that to date there are no experimental studies of temperature distribution on the surfaces of corrugated metal structures. Besides, an assessment of the effect of high and low temperatures on the thermal stress state of transportation facilities made of the CMS has not been conducted. There are also discrepancies regarding taking into account the highest and lowest values of temperatures at the design stage of transportation facilities and their impact on the thermal stress state.

Consequently, it is timely and necessary to undertake the task of an experimental study of temperature distribution on the surfaces of a corrugated metal sheet and to assess the effect of the atmospheric temperature on the thermal stress state of transportation facilities made of the CMS. This will enable engineers of design enterprises to take into account the influence of temperature variations on the stress-strain state of structures at the stage of implementing design works for the construction of transportation facilities from the CMS. Thus, it will help make constructive decisions to reduce this impact on transportation facilities.

3. The aim and objectives of the study

The aim of the study is to determine the effect of climatic temperature fluctuations on the thermal stress state of transportation facilities made of corrugated metal structures.

To achieve the aim, the following tasks were set and done:

– to carry out experimental measurements of the temperature distribution on the surfaces of the corrugated metal sheet;

– to find a solution of the heat conduction problem when setting the temperature values along the contour of the corrugated metal sheet;

– to interpolate the function of temperature by its values on an irregular grid;

– to evaluate the temperature stresses and deformations that arise in corrugated metal sheets of transportation facilities by the finite element method.

4. Experimental measurements of temperature distribution on the surface of a corrugated metal sheet

Temperature distribution was measured by the Testo 875-1 thermal imager and the NT-822 pyrometer (made in Singapore) according to the methods published in the [27, 28]. The atmospheric temperature was monitored using the electronic anemometer TENMARS TM-740. The process of carrying out experimental measurements of temperature is shown in Fig. 1.

Fig. 1. The process of performing temperature measurements on the surface of a corrugated metal sheet of a pipe

When conducting studies on temperature distribution with the aid of a thermal imager on a site, a picture of the temperature distribution on the surfaces of a corrugated metal sheet of a transportation facility made of the CMS was obtained. Then, in laboratory conditions, the temperature distribution was analysed throughout the corrugated structure, using the software Testo-IRsoft. The results of the experimental measurements of the temperature distribution on the boundaries of the corrugated metal sheet are given in Table 1.

Table 1

The experimental results of measuring temperature distribution at the boundaries of a corrugated metal sheet

i	$t_{i,0}$, °C		$t_{i,32}$, °C		j	$t_{0,j}$, °C		$t_{32,j}$, °C	
	summer	winter	summer	winter		summer	winter	summer	winter
0	38.8	–28.8	31.5	–21.5	0	31.4	–21.0	31.0	–21.4
1	38.4	–28.4	31.1	–21.1	1	37.2	–21.4	31.4	–21.4
2	38.8	–28.8	31.4	–21.4	2	30.7	–21.3	31.3	–17.3
3	37.3	–27.3	32.7	–22.7	3	31.5	–21.0	31.0	–20.1
4	37.3	–27.3	31.7	–21.7	4	31.5	–21.4	31.4	–21.5
5	38.2	–28.2	31.0	–21.0	5	31.4	–21.5	31.5	–21.5
6	38.0	–28.0	30.5	–20.5	6	31.7	–21.7	31.7	–21.4
7	38.1	–28.1	29.0	–21.0	7	30.8	–22.3	31.5	–21.7
8	38.1	–28.1	29.9	–20.9	8	32.9	–22.4	32.3	–20.8
9	37.2	–27.2	31.5	–21.5	9	32.0	–23.3	32.4	–22.9
10	36.3	–26.3	30.4	–20.4	10	32.1	–22.9	33.3	–22.0
11	37.4	–27.4	30.8	–20.1	11	32.2	–23.5	32.9	–22.1
12	38.4	–28.4	31.2	–21.2	12	33.4	–23.4	33.5	–22.2
13	38.7	–28.7	32.1	–22.1	13	33.5	–24.4	33.4	–23.4
14	38.7	–28.7	31.2	–21.2	14	31.7	–24.3	34.1	–23.5
15	38.8	–28.8	31.4	–20.4	15	31.4	–24.7	34.3	–21.7
16	38.2	–28.2	31.2	–21.2	16	34.5	–25.5	34.7	–21.4
17	38.0	–28.0	31.1	–20.4	17	34.6	–25.5	35.5	–24.5
18	37,2	–27.2	32.7	–21.1	18	34.7	–26.4	35.5	–24.6
19	38.6	–28.6	32.8	–20.1	19	35.6	–25.4	36.4	–24.7
20	37.2	–27.2	31.7	–22.7	20	34.4	–27.4	35.4	–25.6
21	37.1	–27.1	32.4	–22.8	21	36.0	–27.9	37.4	–24.4
22	38.5	–28.5	31.1	–21.7	22	36.0	–28.9	37.9	–26.0
23	37.6	–27.6	30.5	–22.4	23	36.7	–27.5	38.7	–26.0
24	38.7	–28.7	29.4	–21.1	24	37.1	–27.0	37.5	–26.7
25	38.4	–28.4	30.5	–20.5	25	36.4	–28.0	38.0	–26.5
26	37.1	–27.1	29.4	–19.4	26	37.5	–27.4	37.8	–26.4
27	38.1	–28.1	29.8	–20.5	27	38.0	–27.9	37.8	–27.5
28	37.1	–27.1	31.4	–19.4	28	36.0	–27.4	37.4	–28.0
29	37.4	–27.4	31.0	–19.8	29	38.2	–28.5	38.5	–26.0
30	37.0	–27.0	30.7	–21.4	30	38.1	–28.0	38.0	–28.2
31	37.3	–27.3	31.0	–21.0	31	38.0	–28.8	38.8	–28.1
32	37.4	–27.4	30.4	–20.7	32	38.7	–28.8	38.8	–28.7

Table 1 shows that the temperatures are distributed unevenly throughout the corrugated metal sheet. There is a temperature difference between the lower and upper surfaces of the corrugated metal sheet.

The temperature difference between the lower and upper surfaces of the sheet is +7.1 °C at the highest atmospheric temperatures and −5.5 °C at the lowest atmospheric temperatures.

5. Processing of experimental data on the temperature distribution throughout the surface of the corrugated metal sheet

5. 1. Interpolation of the temperature function by its values on an irregular grid of temperature measurements along the contour of the frame

Let the unknown temperature distribution be in a two-dimensional, single-convex, physically non-homogeneous region P with a piecewise smooth boundary. The set temperature values are in separate points of the region P and at its boundary. On introducing the coordinate system $x0y$ in the region P, the distribution of the temperature field will be determined as a function of the two variables $T(x, y)$.

The task of determining the temperature distribution is incorrect if there are not enough data to write the corresponding boundary conditions for the formulation of the boundary value problem [29]. In this paper, the regularization of an incorrect heat conduction problem is carried out by introducing a physically valid criterion, for choosing from the set of admissible functions the most suitable function for temperature distribution. As a possible criterion for choosing the required function, minimization of the function defined on the set of admissible functions is taken as an integral in the region of the body from the expression given by the entropy production [30]. That is the product of the thermodynamic force on the thermodynamic flow introduced during the consideration of the heat conducting body as a thermodynamic system [31].

The entropy production will be written in the form:

$$\Omega(T)=\iint_P \lambda(x,y)\left[\left(\frac{\partial T(x,y)}{\partial x}\right)^2+\left(\frac{\partial T(x,y)}{\partial y}\right)^2\right]\mathrm{d}x\mathrm{d}y, \quad (1)$$

where $\lambda(x, y)$ is a piecewise constant function in the region P, the coefficient of thermal conductivity of an inhomogeneous body.

Let us write a discrete analogue of the problem of reproducing the temperature function. We apply a regular coordinate grid to the region P with the step h_x in the coordinate x and step h_y in the coordinate y. Let us denote that $T_{i,j}=T(x_i, y_j)$, where $(x_i, y_j)\in P$ are the nodal points of the grid in the region P. It is assumed that at certain points $(x_i^*, y_j^*)\in P$ the temperature values are given, and for the remaining points $(x_i, y_j)\in P$, they are determined from the condition of the minimum of the functional $\Omega(T)$, which after discretization approximates the function:

$$\Omega(T)=\sum_i\sum_j \lambda_{i,j}\left[\left(\frac{T_{i,j}-T_{i-1,j}}{h_x}\right)^2+\left(\frac{T_{i,j}-T_{i,j-1}}{h_y}\right)^2\right]. \quad (2)$$

Note that in this formula there are both given and unknown values of the temperature at the nodal points. In this case, the unknown $T_{i,j}$ can occur four times in sum (2).

$$\Omega(T)=\cdots+\lambda_{i,j}\left(\frac{T_{i,j}-T_{i-1,j}}{h_x}\right)^2+\lambda_{i+1,j}\left(\frac{T_{i+1,j}-T_{i,j}}{h_x}\right)^2+$$
$$+\lambda_{i,j}\left(\frac{T_{i,j}-T_{i,j-1}}{h_y}\right)^2+\lambda_{i,j+1}\left(\frac{T_{i,j+1}-T_{i,j}}{h_y}\right)^2+\cdots.$$

To find a finite number of the unknown temperature values, we use the condition of the minimum of the quadratic function $\Omega(T)$. Let us zero the derivatives of $\Omega(T)$ for the unknown values of $T_{i,j}$ and obtain for each of them the equation:

$$T_{i,j}\left(\frac{\lambda_{i,j}}{h_x^2}+\frac{\lambda_{i+1,j}}{h_x^2}+\frac{\lambda_{i,j}}{h_y^2}+\frac{\lambda_{i,j+1}}{h_y^2}\right)=$$
$$=\frac{\lambda_{i,j}}{h_x^2}T_{i-1,j}+\frac{\lambda_{i+1,j}}{h_x^2}T_{i+1,j}+\frac{\lambda_{i,j}}{h_y^2}T_{i,j-1}+\frac{\lambda_{i,j+1}}{h_y^2}T_{i,j+1}, \quad (3)$$

where $\lambda_{i,j}=\lambda(x_i, y_j)$, and the unknown $T_{i,j}$ is determined by the values in neighbouring nodes, among which there may be known and unknown ones:

$$T_{i,j}=\left(\frac{\lambda_{i,j}}{h_x^2}+\frac{\lambda_{i+1,j}}{h_x^2}+\frac{\lambda_{i,j}}{h_y^2}+\frac{\lambda_{i,j+1}}{h_y^2}\right)^{-1}\times$$
$$\times\left(\frac{\lambda_{i,j}}{h_x^2}T_{i-1,j}+\frac{\lambda_{i+1,j}}{h_x^2}T_{i+1,j}+\frac{\lambda_{i,j}}{h_y^2}T_{i,j-1}+\frac{\lambda_{i,j+1}}{h_y^2}T_{i,j+1}\right). \quad (4)$$

In the case of a homogeneous region P when $\lambda(x, y)=$ $=$const, the formula is simplified to the form:

$$T_{i,j}=\left(\frac{2}{h_x^2}+\frac{2}{h_y^2}\right)^{-1}\left[\frac{1}{h_x^2}\left(T_{i-1,j}+T_{i+1,j}\right)+\frac{1}{h_y^2}\left(T_{i,j-1}+T_{i,j+1}\right)\right], \quad (5)$$

and when $h_x=h_y$, we get the formula:

$$T_{i,j}=\frac{1}{4}\left(T_{i-1,j}+T_{i+1,j}+T_{i,j-1}+T_{i,j+1}\right). \quad (6)$$

Proceeding from some initial approximation of temperature in the region, and hence in the nodes of the regular grid, using formulae (6) and successively changing i, j for the nodes where the values of $T_{i,j}$ are unknown, we organize an iterative process of successive approximation to the desired temperature values. In those nodes where temperature values are set, they remain unchanged.

The calculation process is somewhat different, given that the data may contain errors due to the accuracy extent of the measurements. In this case, we assume that at the measuring points the ranges of possible temperature values are determined, the sizes of which are established by the accuracy of the measurements. If the errors can be either bigger or smaller, then the measured temperature value is located in the middle of the range of its permissible values. In the calculations, we also use formula (6), but we do not allow temperature values to go beyond its permissible values. In this case, it acquires a possible marginal value. Cycle calculations are completed when the next value of the desired temperature in the node differs from the previous less than the given accuracy of the calculations.

The calculation of the temperature field and the stress-strain state of the transportation facility made of the CMS will be carried out at the highest and lowest temperatures obtained as a result of experimental measurements of the temperature distribution throughout the corrugated sheet of the construction.

Due to the small thickness of the sheet construction in comparison with its other dimensions, we neglect the change in temperature in the thickness and also believe that the curvature has little effect on the distribution of temperature on the surface. Thus, to find the temperature distribution, we use the formulae obtained earlier for the measurement of the temperature.

Suppose that for a thin metallic corrugated frame the curvature has a negligible influence on the temperature distribution. Therefore, the calculation of the temperature distribution according to its measurements at the points of the irregular grid on the surface is carried out in an approximation that does not take into account the curvature. To conduct the research, we choose a rectangular area:

$$(P)=\{(x,y):\ 0\le x\le a, 0\le y\le b\}, \qquad (7)$$

where x, y is a rectangular Cartesian coordinate system.

The distribution of the temperature field on the surface of the frame will be carried out with the following parameters: $a=200$ cm; $b=28$ cm and $m=32$. At the points on the boundary of the region (P), we set the experimental values of the temperatures given in Table 1. The values of the highest temperatures were measured on 10 June 2018, at 3.30 p. m., and the lowest temperatures were recorded on 08 January 2019 at about 6.00 a.m. for a fragment of a corrugated metal sheet of a transportation facility that is located in the city of Olesko, Lviv Oblast, Ukraine.

The results of calculating the temperature field by the finite difference method in the software set Mathcad 14 are shown in Fig. 2, *a, b*.

In addition, to compare the results of the distribution of the temperature field, the solution of the heat conduction problem was found by the finite element method, using the licensed program FEMAP (MSC NASTRAN) [32] and taking into account the geometric parameters of the corrugated metal sheet. The results of the temperature distribution on the surfaces of the corrugated metal frame at the highest and lowest atmospheric temperatures are given in Fig. 3, *a, b*.

From the distribution of the temperature field throughout the corrugated metal frame at the highest atmospheric temperatures, it was found that the temperature on the lower surface of the frame varies from +38.8 °C to +37.0 °C. Further, from the bottom up, the temperature gradually decreases to values from + 29.4 °C to 32.7 °C.

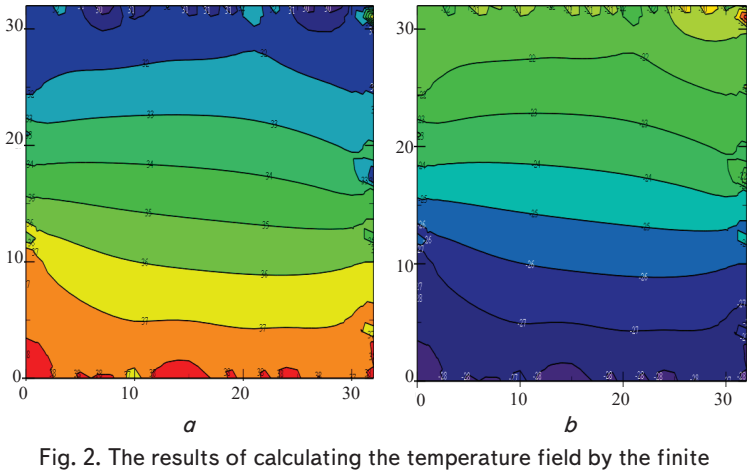

Fig. 2. The results of calculating the temperature field by the finite difference method according to the measured temperatures (°C): *a* — at the highest atmospheric temperatures; *b* — at the lowest atmospheric temperatures

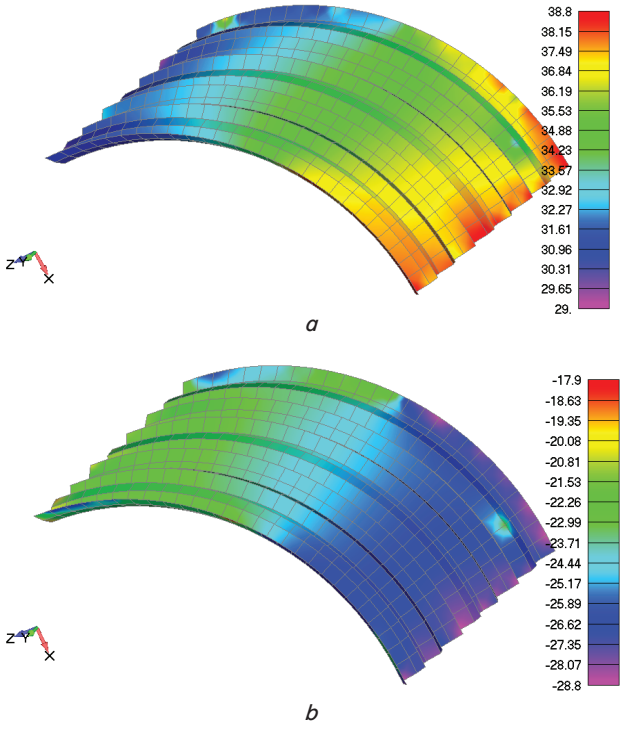

Fig. 3. The results of calculating the temperature field by the finite element method (°C): *a* — at the highest atmospheric temperatures; *b* — at the lowest atmospheric temperatures

At the lowest atmospheric temperatures, the temperature on the bottom surface of the corrugated frame varies from −28.8 °C to −26.0 °C, and the temperature ranges from −19.4 °C to −22.8 °C at the upper boundary of the frame.

After comparing the results of the obtained temperature fields by the finite difference method and the finite element method, it is obvious that the temperature distribution patterns are practically identical. Then, based on the solution of the heat conduction problem, we turn to the determination of the temperature stresses occurring in the corrugated metal frame.

5. 2. Interpolation of the function of temperature by its values on an irregular grid of temperature measurements on the surface of the frame

Let us consider the case of uneven temperature distribution on the surface of the corrugated metal sheet. That is, let us solve the problem of temperature distribution on an irregular grid. At certain nodes of the grid, we set the temperature values that were obtained experimentally at the highest (Fig. 4, *a*) and lowest temperatures (Fig. 4, *b*) of the environment.

By the values of the temperature distribution on the surface of the corrugated metal frame, we solve the heat conduction problem, using finite difference methods and the finite element method. The results of calculating the temperature field by the finite difference method in the software complex Mathcad 14 are shown in Fig. 5, *a, b*, and by the finite element method, the results are given in Fig. 6, *a, b*.

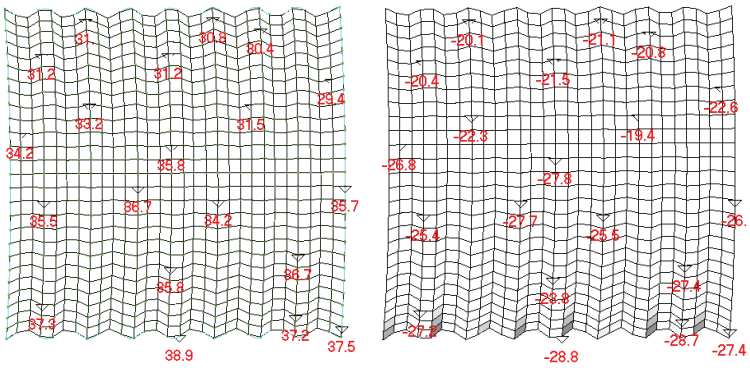

a *b*

Fig. 4. The setting of loads (temperature) on the surface of the corrugated metal frame (°C): *a* — at the highest atmospheric temperatures; *b* — at the lowest atmospheric temperatures

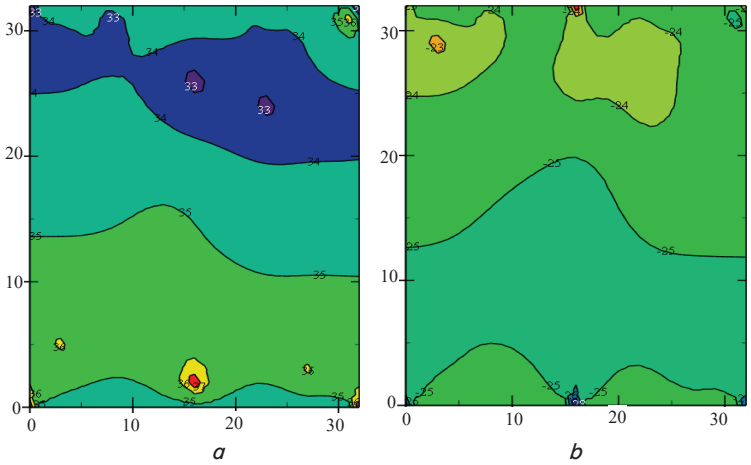

a *b*

Fig. 5. The results of calculating the temperature field by the finite difference method in the uneven temperature distribution throughout the corrugated sheet of the design (°C): *a* — at the highest atmospheric temperatures; *b* — at lowest atmospheric temperatures

From the temperature field (Fig. 5, 6), it is evident that the temperature is distributed unevenly throughout the corrugated metal sheet. At the highest atmospheric temperatures, the temperature on the bottom surface of the corrugated frame varies from +38.8 °C to +36.8 °C, and the temperature values on the upper boundary of the frame range from +29.4 °C to +31.8 °C.

At the lowest atmospheric temperatures, the temperature on the lower surface of the corrugated frame varies from −28.8 °C to −26.3 °C, and the upper surface temperature values range from −19.4 °C to −21.3 °C.

6. The mathematical model of the thermal stress state of a thin frame

A frame is a body bounded by surfaces, the thickness of which is comparable to the other two dimensions. In the theory of thin frames, an orthogonal coordinate system α, β, and γ is predominantly used, where γ is a coordinate that determines the position of the point along the normal to the median surface, and α, β are the coordinates of the points of the median surface. The median surface in the Cartesian coordinate system *Oxyz* is determined by the equations:

$$x = x(\alpha,\beta), \quad y = y(\alpha,\beta), \quad z = z(\alpha,\beta). \tag{8}$$

Thus, the temperature field of the frame can also be given in the coordinate system α, β, and γ. After assuming that the temperature is constant over the thickness of the frame, we assume that $t = t(\alpha,\beta)$, and the temperature in this case depends on the two coordinates.

In the theory of frames, it is considered that the components of the deformation tensor $e_{\gamma\alpha}$, $e_{\beta\gamma}$, and $e_{\gamma\gamma}$ have little effect on the value of other components, so they are set to zero. It is also assumed that the components of the stress tensor $\sigma_{\gamma\alpha}$, $\sigma_{\beta\gamma}$, and $\sigma_{\gamma\lambda}$ slightly affect the stresses $\sigma_{\alpha\alpha}$, $\sigma_{\beta\beta}$, and $\sigma_{\alpha\beta}$. Therefore, the elastic-deformed state is determined by the stresses $\sigma_{\alpha\alpha}$, $\sigma_{\beta\beta}$, and $\sigma_{\alpha\beta}$ as well as the deformations $e_{\alpha\alpha}$, $e_{\beta\beta}$, and $e_{\alpha\beta}$, which are connected by the equations of state:

$$\sigma_{\alpha\alpha} = \frac{E}{1-\nu^2}\left(e_{\alpha\alpha} + \nu e_{\beta\beta}\right) - \frac{\alpha_t E}{1-\nu} t,$$

$$\sigma_{\beta\beta} = \frac{E}{1-\nu^2}\left(e_{\beta\beta} + \nu e_{\alpha\alpha}\right) - \frac{\alpha_t E}{1-\nu} t, \quad \sigma_{\alpha\beta} = \frac{E}{2(1+\nu)} e_{\alpha\beta}. \tag{9}$$

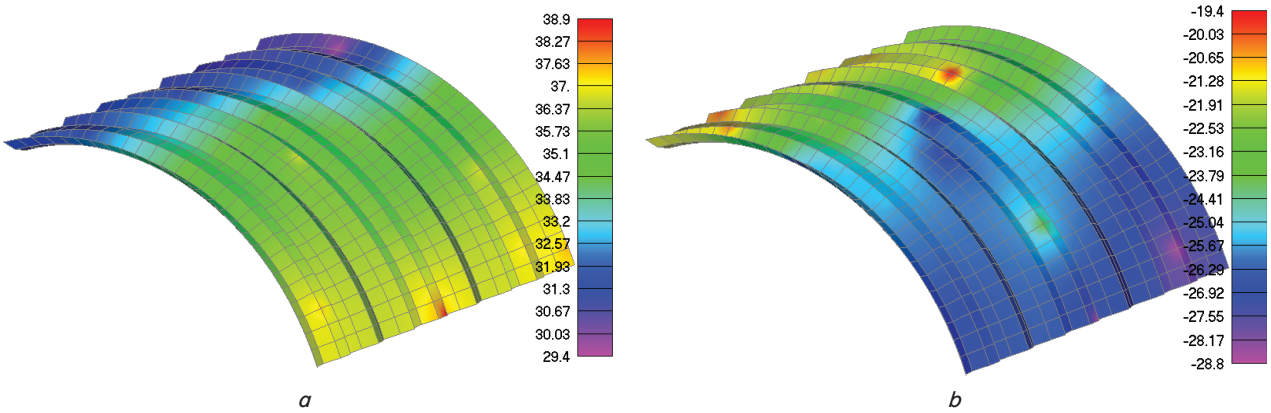

a *b*

Fig. 6. The results of calculating the temperature field by the finite element method in the uneven temperature distribution throughout the corrugated sheet of the structure (°C): *a* — at the highest atmospheric temperatures; *b* — at the lowest atmospheric temperatures

The deformation components $e_{\alpha\alpha}$, $e_{\alpha\beta}$, and $e_{\beta\beta}$ at an arbitrary point of the frame can be represented by the main curvatures of the median surface and the six variables ε_1, ε_{12}, ε_2, κ_1, κ_{12}, and κ_2, which are functions of the two variables α and β of the median surface of the frame, and the expressions for their calculation are given in [33]:

$$e_{\alpha\alpha}=\frac{1}{1+k_1\gamma}\left(\varepsilon_1+\kappa_1\gamma\right),$$

$$e_{\beta\beta}=\frac{1}{1+k_2\gamma}\left(\varepsilon_2+\kappa_2\gamma\right),$$

$$e_{\alpha\beta}=\frac{\left(1-k_1k_2\gamma^2\right)\varepsilon_{12}+2\left(1+k\gamma\right)\kappa_{12}\gamma}{\left(1+k_1\gamma\right)\left(1+k_2\gamma\right)}, \quad (10)$$

where $k=1/2\left(k_1+k_2\right)$ is the average curvature of the median surface of the frame.

Let the coordinate lines of the median surface fall on the boundary of the frame. At the boundaries with the coordinates of the median surface $\alpha=0$ and $\alpha=a$, we have a rigid fastening, and the boundaries $\beta=0$ and $\beta=b$ are free of stresses. Then the boundary conditions, which are given in terms of displacements and tensions, we write in the form:

$$u_\alpha\big|_{\alpha=0}=0,\ u_\beta\big|_{\alpha=0}=0,\ u_\alpha\big|_{\alpha=a}=0,\ u_\beta\big|_{\alpha=a}=0,$$

$$\sigma_\beta\big|_{\beta=0}=0,\ \sigma_{\alpha\beta}\big|_{\beta=0}=0,\ \sigma_\beta\big|_{\beta=b}=0,\ \sigma_{\alpha\beta}\big|_{\beta=b}=0. \quad (11)$$

According to the given algorithm, we will evaluate the stresses that arise in the metal frame on the values of temperature fields, which are shown in Fig. 5, 6.

6. 1. The thermal stress state of the corrugated frame when setting the temperature at the edges of the region

Numerical studies of stresses and deformations are made for the values of the initial parameters that correspond to the geometrical dimensions of the corrugated sheet of the pipe: the length of the corrugation is $a=200$ cm, the width of the eight corrugations is $b=120$ cm, whereas the thickness of the frame of the metallic corrugated sheet is 6 mm, and the radius of the corrugated sheet R is 35 mm. The thermal conductivity of the metal pipe of the MultiPlate MP 150 type is $k=45$ kV/(m·°C), the elastic modulus is $E=2.1\cdot10^5$ MPa, the Poisson coefficient is $\nu=0.3$, and the coefficient of linear temperature expansion is $\alpha=1.25\cdot10^{-5}$ 1/°C. The values of the distribution of the temperature field were those given in the previous subdivision.

Since the analytical solution of thermal elasticity equations (9) and (10) is labour-intensive, the results of the stress-strain state of the corrugated metal frame will be determined by the finite element method, using the licensed software program FEMAP with MSC NASTRAN. Recommendations for calculating corrugated metal structures by the finite element method are given in previous papers [34–39].

The finite-element model of the fragment of the corrugated metal frame is shown in Fig. 7.

The area of the frame is divided into two-dimensional finite elements of the type PLATE in the form of a quadrilateral quadrangle (Fig. 7, *a*).

The number of nodes of the complete elemental model is 810 pieces, which form 754 elements (Fig. 7, *b*).

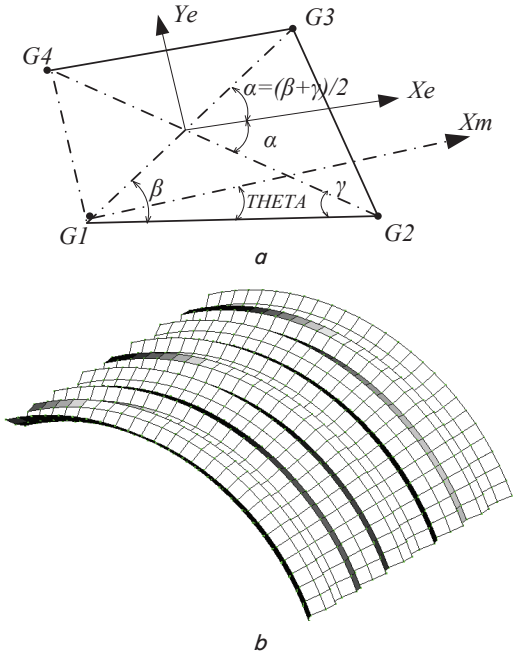

Fig. 7. The finished-element model of a fragment of a corrugated metal frame: *a* — a four-node finite element of the type PLATE; *b* — a finite-element frame decomposition

The results of the distribution of stresses that arise at the highest and lowest atmospheric temperatures are shown in Fig. 8, *a*, *b*.

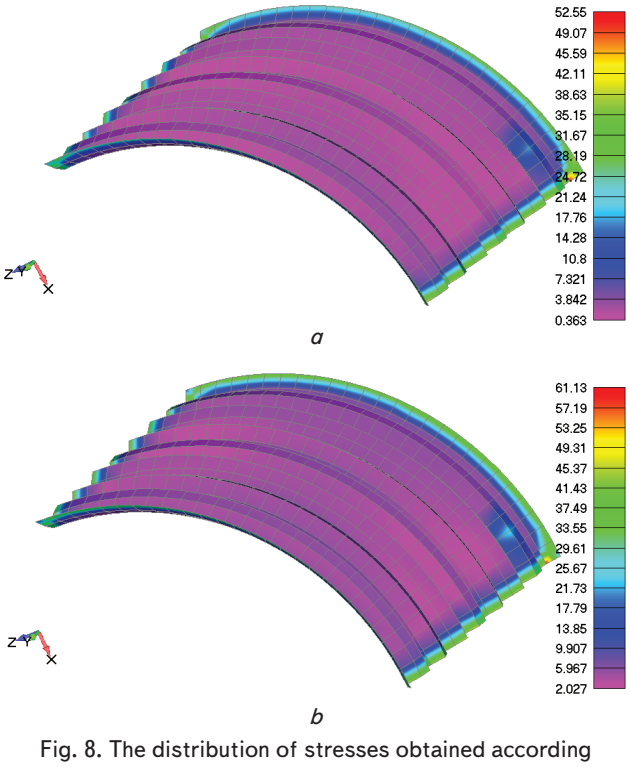

Fig. 8. The distribution of stresses obtained according to Mises's hypothesis throughout the corrugated metal sheet (MPa): *a* — at the highest atmospheric temperatures; *b* — at the lowest atmospheric temperatures

The results of calculating the thermal stress state of the frame indicate that the maximum stress values appear at the

fixed edges of the frame. The values of the stresses occurring in the corrugated metal structure in summer are 52.55 MPa (Fig. 8, *a*), and with the temperature distribution determined by the measured values of temperatures in winter, the temperature stresses are 61.13 MPa (Fig. 8, *b*).

According to the values of the stresses, we calculate deformations of the corrugated metal sheet of a transportation facility that arise in summer and winter (Fig. 9).

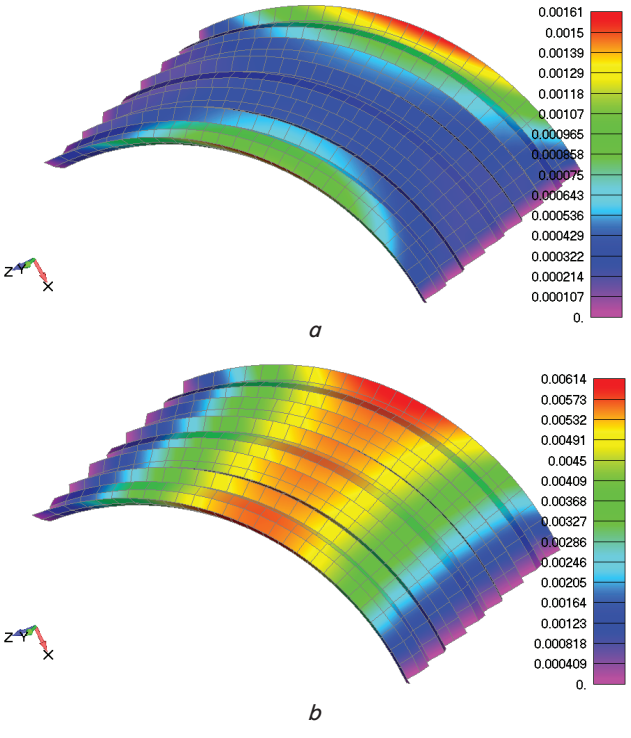

Fig. 9. The distribution of deformations throughout the corrugated metal sheet (mm): *a* — at the highest atmospheric temperatures; *b* — at the lowest atmospheric temperatures

Maximum deformations arise in areas of metal-free corrugated sheets that are load-free. With the measured highest values of summer temperatures, the deformation is $1.61 \cdot 10^{-3}$ mm (Fig. 9, *a*), and at the lowest atmospheric temperatures in winter, the deformation is $6.14 \cdot 10^{-3}$ mm (Fig. 9, *b*).

6. 2. The thermostatic state of the corrugated frame at an uneven distribution of temperatures throughout its surface

The results of the distribution of stresses that arise at the highest and lowest atmospheric temperatures, in the case of setting temperature values only in certain nodes of the grid of finite elements, are shown in Fig. 10, *a, b*.

The values of the stresses occurring throughout the corrugated metal structure in summer are 20.88 MPa (Fig. 10, *a*), and with the temperature distribution determined by the measured values of temperatures in winter, the temperature stresses are 53.94 MPa (Fig. 10, *b*).

The distribution of deformations occurring at a given temperature distribution is shown in Fig. 11.

With positive values of summer temperatures, the deformation is $2.21 \cdot 10^{-4}$ mm (Fig. 11, *a*), and at the lowest atmospheric temperatures in winter, it is $6.87 \cdot 10^{-4}$ mm (Fig. 11, *b*).

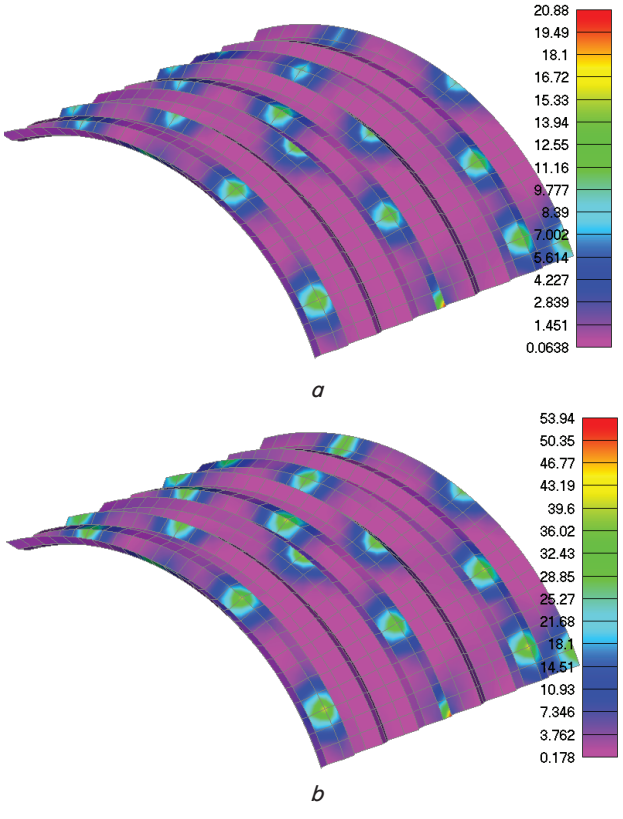

Fig. 10. The distribution of stresses obtained according to Mises's hypothesis throughout the corrugated metal sheet (MPa): *a* — at the highest atmospheric temperatures; *b* — at the lowest atmospheric temperatures

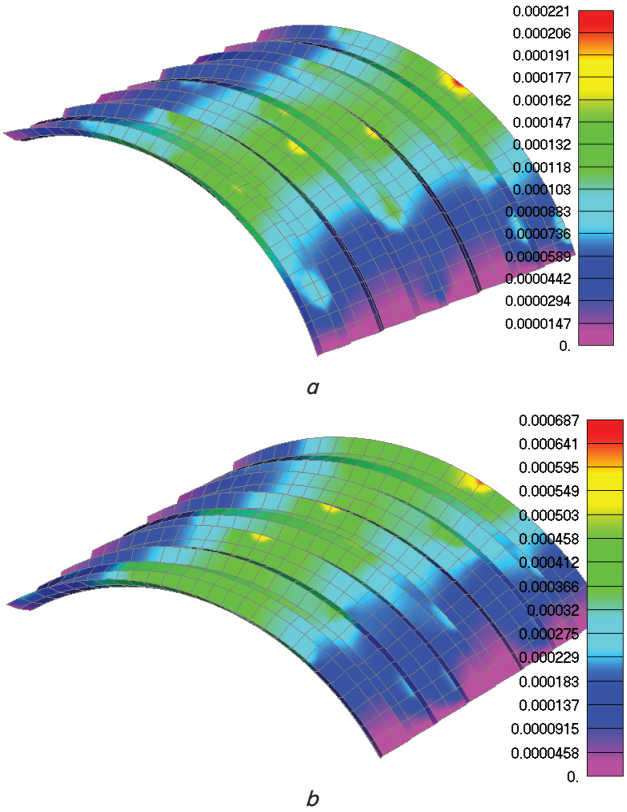

Fig. 11. The distribution of deformations throughout the corrugated metal sheet: *a* — at the highest atmospheric temperatures; *b* — at the lowest atmospheric temperatures

7. Discussion of the results of studying the distribution of temperature fields and the thermal stress state in metallic corrugated structures

When performing experimental studies of temperature distribution throughout a corrugated metal sheet, it was established that the temperature was distributed unevenly in the region of the corrugated sheet. There is a temperature difference between the lower and upper parts of the corrugated metal sheet. This phenomenon is due to the uneven heating of the corrugated sheet of a pipe one side of which is exposed to direct solar radiation while the other side is in the shade.

Besides, the climatic temperature influences have an unstable nature of action. Therefore, when designing corrugated metal structures, it is necessary to consider cases of a rapid decrease in the atmospheric temperature under a clear sky at night until sunrise. In addition, it is necessary to take into account the orientation of the structure in space relative to the sides of the horizon, which has an effect on the unilateral heating of the structure.

The results of calculating temperature stresses and deformations show that when the temperature is determined by the contour of a corrugated metal sheet, the level of temperature stresses is higher than when the temperature is set only in separate nodes of the finite-element model. At the highest temperature values, the level of temperature stresses in the case of setting the temperature in the contour of the sheet is 52.55 MPa, and when given in separate nodes of a finite-element grid, it is 20.88 MPa. The stress difference is 60 %.

At the lowest temperature values, the level of stresses in the case of setting the temperature along the contour of the sheet is 61.13 MPa, and when given in separate nodes of a finite-element grid, it is 53.94 MPa. The difference in the stress values is 12 %.

The results of calculating temperature stresses show that the level of temperature stress does not exceed the permissible limit of 235 MPa of the elasticity of the metal. The temperature stresses make up about 25 % of the permissible stresses, so they should be taken into account when designing transportation facilities made of corrugated metal structures.

When there is one-sided heating of a construction, it is necessary to apply calculations of temperature fields and stresses for a particular day of the year, which approximately corresponds to the conditions of the hottest period. In addition, it is necessary to make calculations of the thermal stress state for the spring period, with a significant difference between the night and daytime air temperature.

One of the disadvantages of conducting studies of temperature fields and stresses occurring in corrugated metal structures is the failure to take into account the temperature distribution in the frame thickness. Therefore, the direction of further research development can involve taking into account the two-sided anti-corrosion coating.

8. Conclusions

1. The experimental tests on the temperature distribution throughout the surface of a corrugated metal sheet have shown an uneven distribution of temperatures throughout the region of the corrugated metal sheet. The temperature difference between the bottom and top sides of the sheet is +7.1 °C at the highest atmospheric temperatures and −5.5 °C at the lowest temperatures. Therefore, when calculating for such structures, it is necessary to take into account the uneven distribution of temperature throughout the surface of the corrugated sheet.

2. The distribution of the temperature field throughout the corrugated metal frame at the highest atmospheric temperatures has revealed that the temperature on the lower surface of the frame varies from +38.8 °C to +37.0 °C. Further, from the bottom up, the temperature gradually decreases to values from +29.4 °C to 32.7 °C.

At the lowest atmospheric temperatures, the temperature on the lower surface of the corrugated frame varies from −28.8 °C to −26.3 °C, and the temperature values at the upper boundary of the frame range from −19.4 °C to −22.8 °C.

3. The stresses caused by atmospheric temperature fluctuations reach the highest values in the case of limiting displacements of the corrugated sheet at the ends. The stresses under given conditions of fastening the corrugated frame are 52.55 MPa at the measured the highest temperatures in summer and 61.13 MPa at the lowest temperature values measured in winter. The level of stresses when combining temperature stresses with stresses from the action of vehicles can lead to premature malfunctioning of corrugated metal structures.

4. The magnitude of the stresses occurring on corrugated metal sheets from the temperature variations in the environment is up to 25 % of the permissible stresses, which emphasizes the need to calculate corrugated metal structures for climatic temperature effects.

References

1. Kovalchuk V. Study of temperature field and stress state of metal convoluted pipes // Resursoekonomni materialy, konstruktsiyi, budivli ta sporudy. 2014. Issue 29. P. 186–192.
2. Machelski Cz. Modelowanie mostowych konstrukcji gruntowo-powlokowych. Dolnoslaskie Wydawnictwo Edukacyjne, 2008. 208 p.
3. Machelski Cz. Kinematic method for determining influence function of internal forces in the steel shell of soil-steel bridge // Studia Geotechnica et Mechanica. 2010. Vol. XXXII, Issue 3. P. 27–40.
4. Pettersson L., Leander J., Hansing L. Fatigue design of soil steel composite bridges // Archives of institute of civil engineering. 2002. Issue 12. P. 237–242.
5. Luchko Y. Y., Kovalchuk V. V. Vymiriuvannia napruzheno-deformovanoho stanu konstruktsiy mostiv pry zminnykh temperaturakh i navantazhenniakh: monohrafiya. Lviv: Kameniar, 2012. 235 p.
6. Mangerig I. Klimatische Temperaturbeanspruchung von Stahl- und Stahlverbundbrucken. Inst. für Konstruktiven Ingenieurbau, Ruhr-Univ., 1986. 143 p.
7. Luchko J., Hnativ Y., Kovalchuk V. Method of calculation of temperature field and deflected mode of Bridge structures in software environment NX Nastran // Theoretical Fuundations of Civil Engineering. 2013. Vol. 21. P. 107–114.
8. Temperature Stresses in Composite Box Girder Bridges / Dilger W. H., Ghali A., Chan M., Cheung M. S., Maes M. A. // Journal of Structural Engineering. 1983. Vol. 109, Issue 6. P. 1460–1478. doi: https://doi.org/10.1061/(asce)0733-9445(1983)109:6(1460)

9. Belyaev V. S., Sandgarten M. L. Metodicheskie osnovy prakticheskih raschetov metallicheskih gofrirovannyh konstruktsiy // Stroymetall. 2009. Issue 1. P. 17–19.
10. Priestley M. J. N., Buckle I. G. Ambient Thermal Response of Concrete Bridges // Bridge Seminar. Vol. 2. 1978.
11. DBN V.2.3-14: 2006. Sporudi transportu. Mosti ta trubi. Pravila proektuvannya. Kyiv, 2006. 359 p.
12. AASHTO Guide specifications: Thermal effects in concrete bridge superstructures. Washington, DC: American Association of State Highway and Transportation Officials, 1989.
13. Rekomendatsii po raschetu temperaturnyh i usadochnyh vozdeystviy na proletnye stroeniya mostov. Odobreny Glavtransproektom. Moscow, 1988. 17 p.
14. EN_1991-1-5-2009. Evrokod 1 vozdeystviya na konstruktsii Chast' 1-5. Obschie vozdeystviya. Temperaturnye vozdeystviya. Ministerstvo arhitektury i stroitel'stva Respubliki Belarus'. Minsk, 2009. 38 p.
15. Metodicheskie rekomendatsii po primeneniyu metallicheskih trub bol'shogo diametra v usloviyah naledeobrazovaniya i mnogoletnemerzlyh gruntov (dlya opytno-eksperimental'nogo stroitel'stva). Moscow, 2003. 65 p.
16. Kovalchyk Y. I. Recommendations of design and construction technology of monolithic post-tensioned concrete bridge spans // SWorld. 2016.
17. Dmytrychenko M. F., Dmytriev M. M., Derkachov O. B. Teplova diahnostyka (osnovy teoriyi ta praktyky zastosuvannia): monohrafiya. Kyiv: NTU, 2012. 168 p.
18. Prikladnaya mekhanika dorozhnyh odezhd na mostovyh sooruzheniyah / Ovchinnikov I. G., Scherbakov A. G., Bochkarev A. V., Naumova G. A. Volgograd: VolgGASU, 2006. 310 p.
19. On the steady-state temperature field of multilayer road pavement / Bogomolov V., Abramchuk F., Raznitzyn I. et. al. // Vestnik HNADU. 2014. Issue 67. P. 94–97.
20. Feng T., Feng S. A Numerical Model for Predicting Road Surface Temperature in the Highway // Procedia Engineering. 2012. Vol. 37. P. 137–142. doi: https://doi.org/10.1016/j.proeng.2012.04.216
21. Design Criteria Skyway Structures. San Francisco-Oakland Bay Bridge East Span Seismic Safety Project, 2001. 91 p.
22. Stankevych V. Z., Butrak I. O., Kovalchuk V. V. Cracks Interaction in the Elastic Composite under Action of the Harmonic Loading Field // 2018 XXIIIrd International Seminar/Workshop on Direct and Inverse Problems of Electromagnetic and Acoustic Wave Theory (DIPED). 2018. doi: https://doi.org/10.1109/diped.2018.8543323
23. De Backer H., Outtier A., Van Bogaert Ph. Numerical and experimental assessment of thermal stresses in steel box girders. Civil Engineering Department, Universiteit Gent, Gent, Belgium NSCC, 2009. P. 65–72.
24. Balmes E., Corus M., Siegert D. Modeling thermal effects on bridge dynamic responses. Ecole Centrale Paris, 2006.
25. Burdet O. L. Thermal Effects in the Long-Term Monitoring of Bridges // IABSE Symposium Report. 2010. Vol. 97, Issue 19. P. 62–68. doi: https://doi.org/10.2749/222137810796025465
26. Sysyn M. P., Kovalchuk V. V., Jiang D. Performance study of the inertial monitoring method for railway turnouts // International Journal of Rail Transportation. 2019. Vol. 7, Issue 2. P. 103–116. doi: https://doi.org/10.1080/23248378.2018.1514282
27. Teplovizor testo 875. Rukovodstvo po ekspluatatsii. URL: https://www.geo-st.ru/upload/iblock/f46/f46af0056a0c67d9b73d5dd617627d85.pdf
28. Pirometr NT-822. Rukovodstvo po ekspluatatsii. 2012.
29. Bek Dzh., Blakuell B., Sent-Kler ml. Nekorrektnye obratnye zadachi teploprovodnosti. Moscow: Mir, 1989. 312 p.
30. Burak Ya., Chaplia Ye., Gera B. Thermodynamic models and investigation methods of heterophase multicomponent systems // XXXV Sympozjon «Modelowanie w mechanice». Gliwice: Politechnika Slaska, 1996. P. 29–34.
31. D'yarmati K. Neravnovesnaya termodinamika. Moscow: Mir, 1974. 304 p.
32. Rudakov K. M. Vstup u UGS Femap 9.3 (dlia Windows). Heometrychne ta skinchenno-elementna modeliuvannia konstruktsiy: pos. Kyiv: NTUU «KPI», 2009. 282 p.
33. Podstrigach Ya. S., Shvets R. N. Termouprugost' tonkih obolochek. Kyiv: Naukova dumka, 1978. 343 p.
34. Kovalchuk V. V. Osnovni zasady rozrakhunku metalevykh hofrovanykh konstruktsiy metodom skinchennykh elementiv pry vzaiemodiyi z hrutovoiu zasypkoiu // Visnyk ODABA. 2014. Issue 56. P. 94–102.
35. Kovalchuk V. Finite-element calculation of stress-strain state of corrugated metal structures in the interaction with soil backfill programmed in NX NASTRAN // Visnyk Lvivskoho natsionalnoho ahrarnoho universytetu. Seriya: Arkhitektura i silskohospodarske budivnytstvo. 2015. Issue 16. P. 19–25.
36. Research and analysis of the stressed-strained state of metal corrugated structures of railroad tracks / Kovalchuk V., Luchko J., Bondarenko I., Markul R., Parneta B. // Eastern-European Journal of Enterprise Technologies. 2016. Vol. 6, Issue 7 (84). P. 4–9. doi: https://doi.org/10.15587/1729-4061.2016.84236
37. The study of strength of corrugated metal structures of railroad tracks / Kovalchuk V., Markul R., Bal O., Milyanych A., Pentsak A., Parneta B., Gajda A. // Eastern-European Journal of Enterprise Technologies. 2017. Vol. 2, Issue 7 (86). P. 18–25. doi: https://doi.org/10.15587/1729-4061.2017.96549
38. Study of the stress-strain state in defective railway reinforced-concrete pipes restored with corrugated metal structures / Kovalchuk V., Markul R., Pentsak A., Parneta B., Gayda O., Braichenko S. // Eastern-European Journal of Enterprise Technologies. 2017. Vol. 5, Issue 1 (89). P. 37–44. doi: https://doi.org/10.15587/1729-4061.2017.109611
39. Estimation of carrying capacity of metallic corrugated structures of the type Multiplate MP 150 during interaction with backfill soil / Kovalchuk V., Kovalchuk Y., Sysyn M., Stankevych V., Petrenko O. // Eastern-European Journal of Enterprise Technologies. 2018. Vol. 1, Issue 1 (91). P. 18–26. doi: https://doi.org/10.15587/1729-4061.2018.123002